LAWRENCE
LIVERMORE
NATIONAL
LABORATORY

LLNL-JRNL-518278

MODELING OF SUDDEN HYDROGEN EXPANSION FROM CRYOGENIC PRESSURE VESSEL FAILURE

G. Petitpas, S. Aceves

December 5, 2011

International of Hydrogen Energy

Disclaimer

MODELING OF SUDDEN HYDROGEN EXPANSION FROM CRYOGENIC PRESSURE VESSEL FAILURE

Petitpas, G. and Aceves, S. M.
Lawrence Livermore National Laboratory,
7000 East Avenue, L-792, Livermore, CA 94550, USA, petitpas1@llnl.gov

ABSTRACT

We have modeled sudden hydrogen expansion from a cryogenic pressure vessel. This model considers real gas equations of state, single and two phase flow, and the specific "vessel within vessel" geometry of cryogenic vessels. The model can solve sudden hydrogen expansion for initial pressures up to 1210 bar and for initial temperatures ranging from 27 to 400 K. For practical reasons, our study focuses on hydrogen release from 345 bar, with temperatures between 62 K and 300 K. The pressure vessel internal volume is 151 Liters. The results indicate that cryogenic pressure vessels may offer a safety advantage with respect to compressed hydrogen vessels because i) hydrogen, when released, discharges first into an intermediate chamber before reaching the outside environment, ii) working temperature is much lower and thus the hydrogen has less energy. Results indicate that key expansion parameters such as pressure, rate of energy release, and thrust are all considerably lower for a cryogenic vessel within vessel geometry as compared to ambient temperature compressed gas vessels. Future work will focus on taking advantage of these favorable conditions to attempt fail-safe cryogenic vessel designs that do not harm people or property even after catastrophic failure of the inner pressure vessel.

1. INTRODUCTION

As a universal transportation fuel that can be generated from water and any energy source, hydrogen (H_2) is a leading candidate to supplant petroleum with the potential to ultimately eliminate petroleum dependence, associated air pollutants and greenhouse gases [1]. The key technical hurdle faced by hydrogen vehicles is packaging enough H_2 onboard the vehicle for an acceptable range. Hydrogen is the lightest molecule (2 g/mol), and faces packaging challenges even when highly pressurized (typically to 350 to 700 bar). Pressures beyond 700 bar are not used in transportation since hydrogen becomes increasingly incompressible with pressurization [2].

Liquid hydrogen (LH_2) vessels store hydrogen at 20-30 K and 1-6 bar [3], at considerably higher density than ambient temperature pressurized H_2 (70.77 kg/m^3 at 20.3 K and 1 bar vs. 39 kg/m^3 at 300 K and 700 bar). The main drawback of LH_2 storage is extreme sensitivity to environmental heat transfer. Very high performance insulation (~1 Watt total heat transfer) is necessary for avoiding rapid hydrogen evaporation and pressurization that forces hydrogen release to avoid exceeding the vessel pressure rating. These venting, or "boil-off" losses, may be substantial when the vehicle is not driven frequently.

Cryogenic pressure vessels [4][5][6] have been proposed as a solution to the LH_2 boil-off problem. Rated for much higher pressures (~345 bar vs. 6 bar in LH_2 vessels), cryogenic pressure vessels contain the hydrogen even as it evaporates and pressurizes. As a consequence, the time before venting is needed (dormancy) increases considerably. Expansion work cools down the vessel when hydrogen is extracted, and therefore even short driving distances (~10 km/day) are sufficient for eliminating evaporative losses. Cryogenic pressure vessels take advantage of the high density of liquid hydrogen without losing any to evaporation during regular use, therefore enabling compact H_2 storage systems that require considerably less carbon fiber than compressed gas tanks, with a consequent reduction in overall system cost [7].

Cryogenic pressure vessels comprise a high-pressure inner vessel made of carbon-fiber-coated aluminum (similar to those used for storage of compressed gas), a vacuum space filled with numerous sheets of highly reflective plastic (for high performance thermal insulation), and an outer metallic jacket (Fig. 1). Cryogenic pressure vessels may typically be filled with cryogenic hydrogen for high storage capacity. However, ambient temperature compressed gas can also be used e.g., if cryogenic hydrogen is not available in the early stages of infrastructure development.

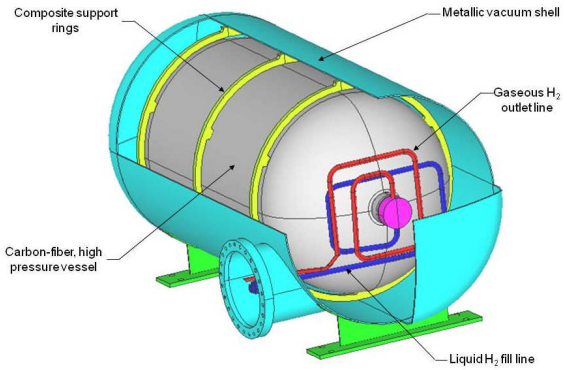

Figure 1. Cryogenic vessel within vessel configuration. Inner vessel is an aluminum-wound, carbon fiber-wrapped pressure vessel similar to those typically used for storage of compressed gases. This vessel is surrounded by a vacuum space filled with numerous sheets of highly reflective plastic (minimizing heat transfer into vessel), and an outer metallic vacuum jacket.

Aside from volume, weight cost, and refueling advantages [8], cryogenic pressure vessels offer safety advantages because of their low temperature and geometry. Figure 2 shows the theoretical mechanical energy released by a sudden adiabatic expansion to atmospheric pressure (e.g. in a vessel rupture) of high-pressure hydrogen gas from three temperatures (80 K, 150 K and 300 K). H_2 stored at 70 bar and 300 K will release a maximum mechanical energy of 0.55 kWh/kg if suddenly (i.e. adiabatically) expanded to atmospheric pressure (cooling substantially). Counterintuitively, this maximum energy release increases only slightly with much higher H_2 pressures. Raising vessel pressure to 1000 bar (1400% increase from 70 bar) increases maximum mechanical energy release by only 10% while shrinking vessel volume and strengthening (thickening) vessel walls many times over.

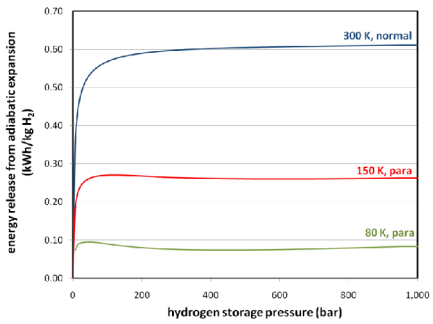

Figure 2. Maximum mechanical energy (per kilogram of hydrogen) released upon instantaneous expansion of H_2 gas as a function of initial storage pressure at 80 K, 150 K, and 300 K. For comparison, note that the chemical energy content of hydrogen is 33.3 kWh/kg. This mechanical energy is the theoretical maximum available work based on reversible adiabatic expansion from the pressure shown to 1 atm, calculated from internal energy differences of H_2 gas before and after isentropic expansion [6].

The vacuum jacket surrounding a cryogenic pressure vessel (Fig. 1) also contributes to safety by offering a second layer of protection, eliminating environmental impacts over the life of the pressure vessel and providing expansion volume to mitigate shocks from hydrogen release. If the inner pressure vessel were to catastrophically break, it would be possible for the vacuum jacket to contain the hydrogen expansion and shrapnel (if any). Subsequent operation of the vacuum vessel pressure relief device (e.g., rupture disk) would limit vacuum vessel pressurization, and may conduct to harmless hydrogen venting.

The synergy between low burst energy and vessel within vessel construction may be used in the future to build fail-safe cryogenic vessels that do not harm occupants or damage property even when the inner vessel fails catastrophically. While much research is still necessary to demonstrate this possibility, we now present as a first step a calculation of hydrogen release during sudden vessel failure. Future work may then use these results for evaluating system characteristics (vacuum vessel thickness and design, rupture disk area) for maximum safety.

2. LITERATURE SURVEY

Sudden release from ambient temperature compressed hydrogen vessels has been studied multiple times. Different levels of complexity have been used, with models going from 1D [9], to 2D axisymetric [10-11-12] and 3D [13], and pressure ranging from 100 bar [14] to 1000 bar [10]. Mohamed *et al* [9] compared 1D and 3D models for describing hydrogen release inside the vessel and at the throat. Good agreement was found between the two. Researchers agree that flow cannot be accurately simulated with ideal gas equation of state for initial tank pressures of more than 100 bar [13], [15]; a real gas model is therefore required. Beattie-Bridgeman [9], [12]-[13] and Abel Noble [15] real gas equations have been compared with ideal gas formulation. Khaksarfad *et al* [13] found negligible discrepancies between the two formulations. Dispersion of hydrogen into the environment during the high-pressure release has also been studied [13]-[15].

In contrast with ambient temperature expansion, *cryogenic* H_2 expansion remains relatively unexplored. Cryogenic expansion calculations are challenging for at least three reasons. First, hydrogen is initially much colder and is therefore more likely to undergo phase change (condensation) during expansion. Second, the geometry of cryogenic pressure vessels is different from ambient temperature vessels because the hydrogen that leaves the vessel first runs through an expansion chamber (vacuum jacket) before its release into the atmosphere. Finally, equilibrium H_2 at low temperature has different composition of para and ortho nuclear spin arrangements than H_2 at room temperature (normal hydrogen), and para and ortho phases expand differently because they have different specific heats and internal energies as a function of temperature [16]. Maytal *et al* [17], [18] calculated expansion conditions for stagnation states initially near and slightly above the critical point, for various species including H_2. Choking states were determined for stagnation temperatures above the thermodynamic critical temperature and discussed as a function of different reduced parameters.

This paper aims at developing a detailed thermodynamic model of sudden hydrogen release from cryogenic pressure vessels. At first, critical flow around and inside the two-phase dome is calculated. Real gas equations are used and choked conditions at the throat are calculated for any stagnation state around the two-phase dome, down to 0.7 times the critical thermodynamic temperature. This modeling capability is then used in the second part of the article to characterize hydrogen release from compressed and cryogenic vessels.

3. CHOKED FLOW FOR REAL AND 2-PHASE FLUIDS

In single-phase, choked flow is determined by either maximizing the flow rate with respect to throat pressure or by comparing the velocity to the local speed of sound. The choking state matches the velocity with the local speed of sound (its Mach number is equal to 1). For two-phase choking states, the speed of sound is not directly predictable and the first definition is therefore used: for given initial stagnation conditions the mass flow at the throat is maximized for one set of conditions along the

isentropic curve. The stagnation point and the throat have the same entropy, and one intensive physical property (such as pressure, temperature or density) is varied in order to maximize the mass flow G, defined as:

(1)

where h - specific stagnation enthalpy; h_t - specific enthalpy at the throat; ρ- density at the throat.

The methodology demonstrated above enables calculation of throat conditions for any stagnation point over the whole hydrogen gas-liquid domain. We next show the H_2 choking states for inside the 2-phase dome (Figure 3). The equations of state are derived from REFPROP Version 8.0 [19]. No slip is considered between the gaseous and the liquid phase (the two phases have the same velocity). At "A", both the stagnation point and the throat are single phase fluids (throat is at 1 bar, 23.9 K, and stagnation is 2 bar, 32.9 K). At "B", the stagnation point is still single phase, but the hydrogen at the throat is on the saturated gas curve (q=1). At "C", the stagnation point is single phase and the hydrogen becomes two phase (q<1) at the throat (same stagnation temperature for A, B, C, and D). At "D", the stagnation point is single phase and the hydrogen at the throat is on the saturated liquid curve (q=0); the curve "θ = 1" exits the two-phase throat dome. At "E", the stagnation point is gas saturated, and the throat is two phase. Similarly, the stagnation point at "F" is liquid saturated and the throat is two phase.

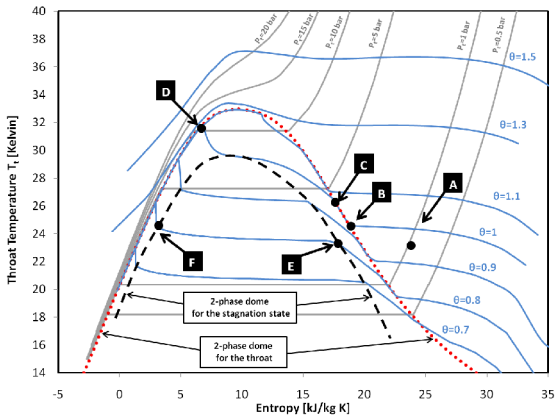

Figure 3. Trajectories of choking states of homogenous flow near the two-phase dome. Blue trajectories "θ" are the isothermal groups of stagnation-reduced temperature (ratio between the stagnation temperature and the thermodynamic critical temperature). T_t and P_t are the throat temperature and pressure, respectively. The red dotted curve is the 2-phase dome for the throat, while the black dashed curve is the 2-phase dome for the stagnation state.

We now assume an isentropic expansion. Two cases of isentropic expansion are studied: (1) the stagnation state has a high initial entropy (higher than the thermodynamic critical entropy ~ 10 kJ/kgK), and then the throat state would enter the two-phase dome (red dotted line) on the right hand side, where the phase change starts with q=1 (saturated gas side); and (2) the stagnation state is initially at low entropy (lower than the thermodynamic critical entropy), and the expansion would enter the two phase dome on the left hand side, where the fluid at the throat becomes first saturated liquid . The "high" entropy example is chosen to be 15 kJ/kg K while the "low" entropy is 5 kJ/kg K. Both expansions are represented as throat pressure, velocity, and quality versus stagnation pressure, where the X-axis is in reverse order (decreasing stagnation pressure from left to right).

At "high entropy" (Figure 4), the flow is first single phase at both the throat and stagnation points. Between 17 and 14 bar, the flow becomes gas saturated (q=1) at the throat: as previously seen, velocity then abruptly decreases. Even though the throat pressure appears to be constant during that phase, computation shows that it decreases slightly (about 0.06 bar). Temperature and density are not

represented here but follow the same path as pressure: decreasing as the stagnation pressure drops, until the throat saturates, where the values remain almost constant, then decreasing as the quality at the throat decreases from unity. Furthermore, the phase change at the stagnation state does not have a significant impact on the expansion. Finally, both phase changes begin at q=1, through the gas saturated line, for the "high" entropy case.

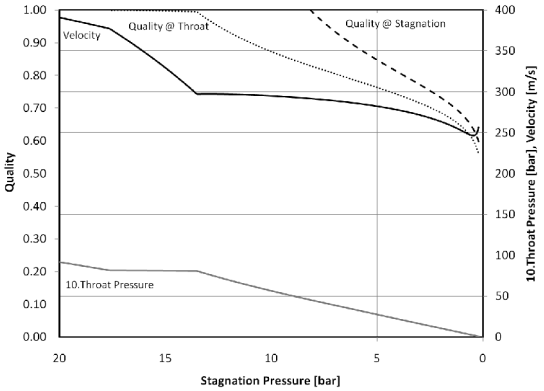

Figure 4. Throat velocity, pressure, and quality of the choking states of hydrogen along the isentropic trajectory s=15 kJ/kg K (high entropy), as function of the stagnation pressure (reverse order).

At "low" entropy (5 kJ/kg K, Figure 5), the flow at the throat saturates at higher stagnation pressure than the previous regime (about 170 bar vs. 17 bar). The throat pressure (as well as throat density and temperature) experiences a longer "plateau" until the throat quality leaves the liquid saturated line (at about 10 bar). At that point, the throat density decreases as the quality increases, and thus the throat velocity increases. We can notice the difference in magnitude and behavior for the velocity between Figures 4 and 5: at "low" entropy, the velocity at the throat is insensitive to the transition from single to two phase at the throat when reaching saturation (q=0), around 170 bar.

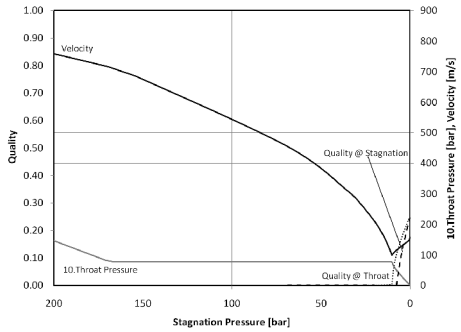

Figure 5. Throat velocity, pressure, and quality of the choking states of hydrogen along the isentropic trajectory s=5 kJ/kg K (low entropy), as a function of the stagnation pressure (reverse order).

4. CRYOGENIC PRESSURE VESSEL HYDROGEN RELEASE MODEL

The models for single and two phase choked flow are now applied to analyzing sudden cryogenic vessel failure, where hydrogen vents through a throat (e.g., a broken tube or a bullet hole) into the vacuum jacket where the pressure will build up until reaching the rupture disc setting (1.3 bar) to finally release into the atmosphere (Figure 6). Sonic conditions are thus calculated at the throat and at the rupture discs (between the vacuum jacket and the atmosphere). The main dimensions of the cryogenic pressure vessel are listed in Table 1.

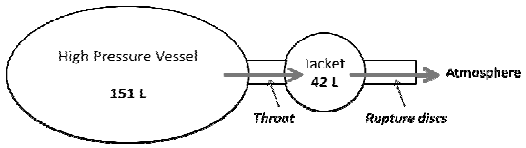

Figure 6. Schematic of the hydrogen release model for the cryogenic pressure vessel

Table 1. Surfaces and volumes of the cryogenic pressure vessel [6].

S_{throat}	$S_{rupture.discs}$	V_1 (pressure vessel)	V_2 (jacket)
0.45 cm^2	19.1 cm^2	0.151 m^3	0.042 m^3

The total surface area of the throat between the pressure vessel and the jacket is 0.45 cm^2. This area corresponds to a 7.62 mm diameter hole, equal to the bullet caliber necessary for pressure vessel certification [23].

A lumped model was used, assuming that hydrogen in each vessel is at a uniform temperature and pressure. We now write the equations for conservation of mass and energy for both the pressure vessel and the vacuum jacket, where the subscripts 1 and 2 denote the pressure vessel and the vacuum jacket, respectively. The subscripts t and d refers to the throat and the rupture discs.

In the pressure vessel:

Conservation of mass

— (4)

Conservation of energy

—— (5)

In the jacket:

Conservation of mass

— (6)

Conservation of energy

—— (7)

where V – volume; t- time; ρ - density; a-velocity; u and h - specific internal energy and enthalpy.

We also consider the following simplifying assumptions:

- Hydrogen release is adiabatic; no heat transfer occurs between the gas and containers
- The orifice is at choked condition (i.e., the gas velocity at the orifice is equal to the local speed of sound) throughout the process. This assumption yields conservative results because in reality, the flow becomes subsonic once the pressure in the vessel falls below a critical pressure, reducing flow rate and the energy of the jet while lengthening the venting process.
- Expansion of hydrogen from stagnation state inside the chamber to choked state at the orifice takes place at a small region near the orifice and is modeled by a quasi one-dimensional isentropic flow.

- The calculation ends when the vacuum jacket reaches atmospheric pressure.
- Real gas behavior is modeled with REFPROP Version 8.0 [19].

5. RESULTS

We present results for room temperature compressed gas vessels (today's technology for automotive H_2 storage) and cryogenic vessels to establish a direct comparison that may indicate their relative safety advantages. We assume that the pressure vessel is at 345 bar when the release initiates. Initial conditions are listed in Table 2. It can be seen that the two cases (room temperature compressed hydrogen storage and cryogenic compressed hydrogen) fall within the two different entropy regimes previously described in this paper. The first *room temperature* case is "high" entropy (> 10 kJ/kg K) while the second *cryogenic* case is low entropy (< 10 kJ/kg K). Patterns similar to Figures 4 and 5 will thus be observed. In the jacket chamber, the "high" entropy pattern will be observed for both cases (entropy = 109 kJ/kg K)

Table 2. Initial condition for the main calculations

	Room temperature compressed hydrogen	**Cryogenic compressed hydrogen**
P_1 (t=0) [bar]	345	345
P_2 (t=0) [millitorr]	1	1
T_1(t=0) [K]	300	62
T_2(t=0) [K]	300	62
ρ_1(t=0) [kg/m^3]	22.9	70.7
Entropy 1 [kJ/kg.K]	32.53	7.37
Entropy 2 [kJ/kg.K]	109	109

At t = 0 s, a 7.62 mm diameter hole opens between the high-pressure vessel and the vacuum jacket. From the initial conditions in Table 2, we apply standard numerical methods to integrate the equations of conservation of mass and energy. A 0.002 s time step was determined appropriate by observing little sensitivity in the solution when smaller values were used.

Figure 7 shows pressure history in the vessel and the vacuum jacket in the case of a sudden hydrogen release from 345 bar and 300 K. The release lasts for about 5 seconds, during which the hydrogen in the pressure vessel cools down to 50 K. The maximum pressure in the vacuum jacket is 15.4 bar. The advantage of the vessel within vessel design is clearly illustrated here, as expansion to the atmosphere occurs from a much lower pressure (the jacket instead of the pressure vessel). The history in the vacuum jacket is presented here to show the effect of a second container around the pressure vessel. A single room temperature pressure vessel does not experience phase change at any time.

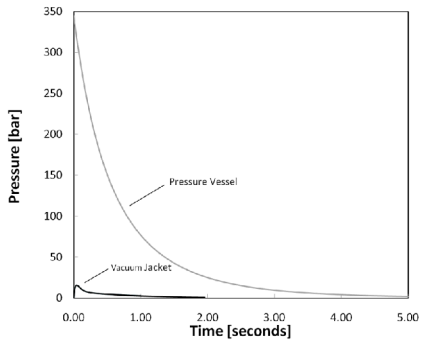

Figure 7. Pressure inside the vessel and vacuum jacket during a sudden hydrogen release from 345 bar, 300 K.

Figure 8 shows a detail of the first second of the sudden expansion from 345 bar and 300 K. The figure shows pressure, temperature and density inside the pressure vessel, at the throat, in the vacuum jacket and at the rupture discs (top to bottom). The mass flow rate is calculated at the throat and rupture discs. Again, we notice the advantage of the vessel within vessel configuration vs. the single vessel: pressure at the rupture discs is lower than throat pressure by ~2 orders of magnitude. Temperature in the vacuum jacket and rupture discs rapidly becomes cryogenic. As a consequence, a phase change is observed at the rupture discs at about 0.5 seconds, which explains the non-monotonic pressure behaviour.

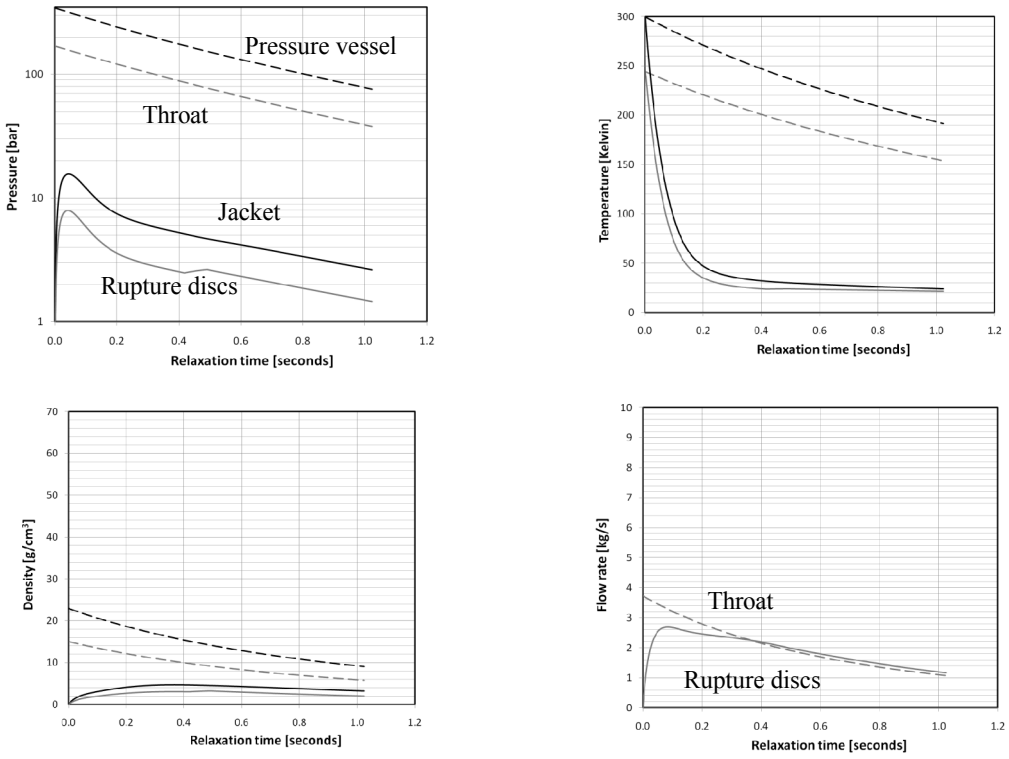

Figure 8. Pressure (logarithmic scale), temperature, density and flow rate versus time; for hydrogen release from 345 bar, 300 K.

Figure 9 shows the pressure and quality history in the vacuum jacket and at the rupture discs. Hydrogen in the vacuum jacket starts condensing after 1 second, and the maximum pressure at the system's outlet is around 8 bar vs. 170 bar for a single vessel.

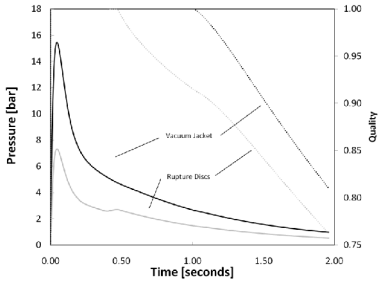

Figure 9. Pressure and quality (vapor mass fraction) in the vacuum jacket and at the rupture discs for a hydrogen release from a pressure vessel at 345 bar and 300 K.

Figure 10 shows the results for a sudden expansion from a vessel at 345 bar and 62 K. The worst-case scenario is considered here: an initially full tank at the maximum rated pressure and very high density (70.7 kg/m^3). Pressure, temperature and density are calculated inside the pressure vessel, at the throat, in the vacuum jacket and at the rupture discs. Mass flow is calculated at the throat and rupture discs. The two vessels are initially at two different "patterns" of entropy, as described earlier: initial entropy in the pressure vessel is low while entropy in the vacuum jacket is high. As a consequence, two different behaviors are observed. Pressure (as well as temperature and density) at the throat experiences a "plateau" as the hydrogen enters the liquid saturated state (at about 0.4 s). It then decreases with time as the quality at the throat becomes greater than zero.

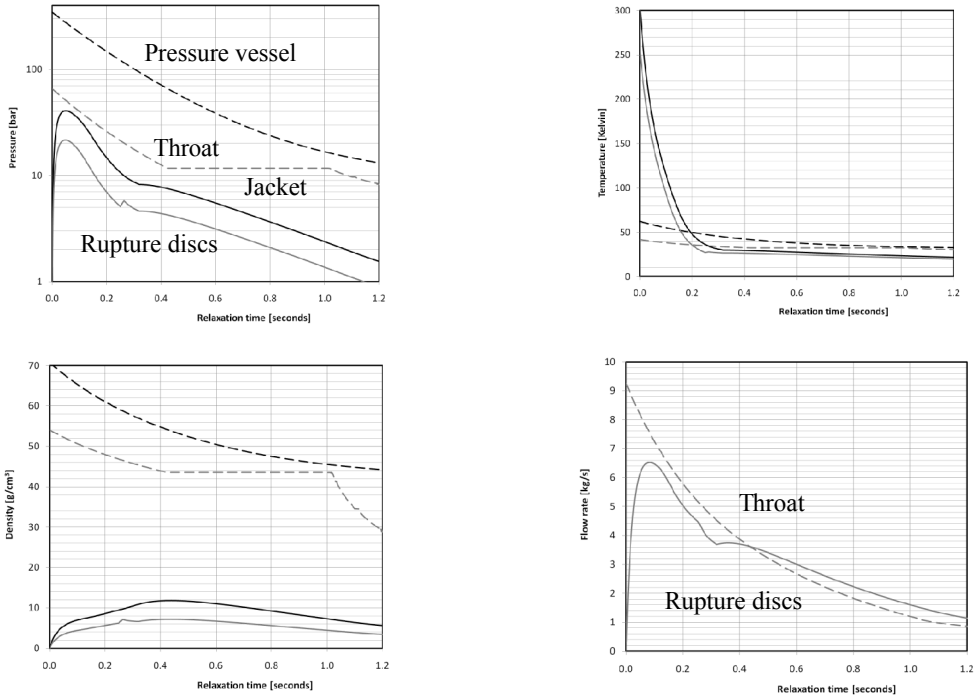

Figure 10. Pressure (logarithmic scale), Temperature, Density and Flow Rate versus time for hydrogen release from a cryogenic vessel initially at 345 bar, 62 K.

6. SAFETY

We now look at how energy is released from the storage system. Among the different criteria, we choose thrust and released power at the outlet. The two parameters are defined below:

— (8)

(9)

where v - velocity at the throat, m/s; G - flow rate, kg/s; S - throat area,m^2; P_t - pressure at the throat, Pa; P_d - pressure downstream the throat, Pa; d - density at the throat, kg/m^3.

Three different cases are presented here to emphasize the importance of the vessel within vessel configuration: room temperature single vessel, room temperature vessel within vessel and cryogenic vessel within vessel (typical cryogenic configuration). Pressure, thrust and released power are calculated at the outlet flow boundary (throat for pressure vessel and rupture disk for vacuum jacket) where hydrogen diffuses into the surroundings potentially harming people or property.

Figures 11 and 12 show thrust and released power divided by the mass of H_2 initially stored (in kg). Trends are similar for the two figures: the cryogenic case exhibits the safest values (lowest thrust and released power), and the 300 K vessel within vessel case exhibits similar values to the cryogenic case. Once again, this highlights the advantage of releasing first in a secondary chamber (the vacuum jacket), which acts as an energy buffer. In 1 second, a room temperature vessel would release 149 Wh/kg H_2, while the cryogenic vessel would release 15.35 Wh/kg H_2 over the same period of time.

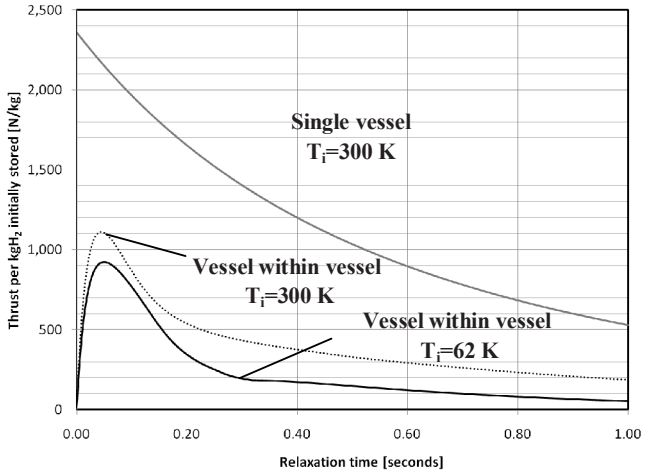

Figure 11. Thrust per kg of stored H_2 as function of time, for a 300 K compressed gas tank (no vacuum vessel), a 300 K vessel within vessel, and a vessel within vessel initially at 62 K.

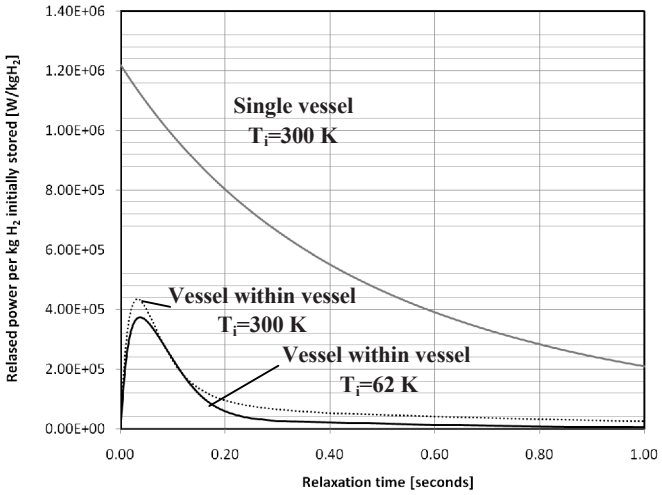

Figure 12. Energy released per second per kg of stored H_2 as function of time for a 300 K compressed gas tank (no vacuum vessel), a 300 K vessel within vessel, and a vessel within vessel initially at 62 K.

7. CONCLUSIONS

We have developed a model for sudden hydrogen expansion from a cryogenic pressure vessel. The purpose is evaluating safety characteristics and potential advantages of low temperature operation and vessel within vessel construction (Fig. 1). The model considers real gas equations of state, and single and two phase flow, and has been used over a wide range of conditions of interest to cryogenic pressure vessels: 62-300 K and up to 350 bar.

The first part of the paper focuses on expansion through the liquid-vapor region of the phase diagram. It has been noticed that two patterns are usually met. If the entropy of the stagnation point is “low”

(typically <10 kJ/kg K, the entropy at the thermodynamic critical point), the discharge will occur at low velocity and the quality of the mixture will increase from the liquid saturation state (q=0). If the entropy of the stagnation point is "high" (>10 kJ/kg K), the discharge will be faster and the quality of the mixture will decrease from the gas saturation state (q=1). The "low entropy" case will have a higher mass flow than the "high entropy" because it is generally at higher density.

The second part applies the theoretical model to the calculation of accidental releases of hydrogen from cryogenic and compressed gas vessels. Results indicate that in the event of an accidental release, a 151 L vessel starting at 345 bar and 300 K would vent down to near atmospheric pressure in about 5 seconds, with 173 bar maximum pressure and 4 kg/s flow rate at the vessel outlet. On the other hand, the same vessel initially at 345 bar and 62 K would vent to near atmospheric pressure in less than 2 seconds, with 22 bar maximum pressure and 6.2 kg/s flow rate at the vessel outlet. Furthermore, the maximum energy released over the first second would be almost 10 times lower for a cryogenic vessel than for a room temperature vessel (149 Wh/kg H_2 vs. 15.35 Wh/kg H_2).

Cryogenic pressure vessels may offer a safety advantage with respect to compressed hydrogen vessels because i) hydrogen, when released, discharges first into an intermediate chamber before reaching the outside environment, ii) working temperature is much lower and thus the hydrogen has less energy. Results indicate that key expansion parameters such as pressure, rate of energy release, and thrust are all considerably lower for a cryogenic vessel within vessel geometry as compared to an ambient temperature compressed gas vessels.

Similarly to the approach performed in the literature for room temperature tanks, future work should include 2D axisymetric or 3D simulation of the hydrogen release inside the vessel (including a comparison with results presented here), and simulations of hydrogen release into the atmosphere. Future work should also include model validation with high-speed pressure and temperature data.

ACKNOWLEDGMENTS

This project was funded by DOE, Office of Fuel Cell Technologies, Antonio Ruiz, Technology Development Manager. This work performed under the auspices of the U.S. Department of Energy by Lawrence Livermore National Laboratory under Contract DE-AC52-07NA27344.

REFERENCES

[1] G. D. Berry and S. M. Aceves, "The Case for Hydrogen in a Carbon Constrained World," *Journal of Energy Resources Technology*, vol. 127, no. 2, pp. 89-94, Jun. 2005.

[2] S. Maus, J. Hapke, C. N. Ranong, E. Wüchner, G. Friedlmeier, and D. Wenger, "Filling procedure for vehicles with compressed hydrogen tanks," *International Journal of Hydrogen Energy*, vol. 33, no. 17, pp. 4612-4621, Sep. 2008.

[3] T. Wallner et al., "Fuel economy and emissions evaluation of BMW Hydrogen 7 Mono-Fuel demonstration vehicles," *International Journal of Hydrogen Energy*, vol. 33, no. 24, pp. 7607-7618, Dec. 2008.

[4] S. M. Aceves, G. D. Berry, and G. D. Rambach, "Insulated pressure vessels for hydrogen storage on vehicles," *International Journal of Hydrogen Energy*, vol. 23, no. 7, pp. 583-591, Jul. 1998.

[5] S. M. Aceves, G. D. Berry, J. Martinez-Frias, and F. Espinosa-Loza, "Vehicular storage of hydrogen in insulated pressure vessels," *International Journal of Hydrogen Energy*, vol. 31, no. 15, pp. 2274-2283, Dec. 2006.

[6] S. M. Aceves et al., "High-density automotive hydrogen storage with cryogenic capable pressure vessels," *International Journal of Hydrogen Energy*, vol. 35, no. 3, pp. 1219-1226, Feb. 2010.

[7] R. K. Ahluwalia et al., "Technical assessment of cryo-compressed hydrogen storage tank systems for automotive applications," *International Journal of Hydrogen Energy*, vol. 35, no. 9, pp. 4171-4184, May 2010.
[8] R. K. Ahluwalia, T. Q. Hua, J.-K. Peng, and R. Kumar, "System Level Analysis of Hydrogen Storage Options," presented at the 2010 DOE Hydrogen Program Review, 2010 DOE Hydrogen Program Review, Washington, DC, 2010.
[9] K. Mohamed and M. Paraschivoiu, "Real gas simulation of hydrogen release from a high-pressure chamber," *International Journal of Hydrogen Energy*, vol. 30, no. 8, pp. 903-912, Jul. 2005.
[10] M. I. Radulescu and C. K. Law, "The transient start of supersonic jets," *Journal of Fluid Mechanics*, vol. 578, p. 331, Apr. 2007.
[11] F. Péneau, G. Pedro, P. Oshkai, P. Bénard, and N. Djilali, "Transient supersonic release of hydrogen from a high pressure vessel: A computational analysis," *International Journal of Hydrogen Energy*, vol. 34, no. 14, pp. 5817-5827, Jul. 2009.
[12] Y.-F. Liu, N. Tsuboi, H. Sato, F. Higashino, and A. K. Hayashi, "Direct numerical simulation on hydrogen fuel jetting from high pressure tank," presented at the 20th International colloquium on the Dynamics of Explosions and Reactive Systems (ICDERS), Montreal, Canada, 2005.
[13] R. Khaksarfard, M. R. Kameshki, and M. Paraschivoiu, "Numerical simulation of high pressure release and dispersion of hydrogen into air with real gas model," *Shock Waves*, vol. 20, no. 3, pp. 205-216, May 2010.
[14] Pedro, G., Penau, F., P. Oshkai, and N. Djilali, "Computational Analysis of Transient Gas Release from a High Pressure Vessel," presented at the CFDSC 2006, Kingston, Canada, July, 16-18.
[15] Z. Cheng, V. M. Agranat, A. V. Tchouvelev, W. Houf, and S. V. Zhubrin, "PRD hydrogen release and dispersion; a comparison of CFD results obtained from using ideal and real gas law properties," presented at the International Conference on Hydrogen Safety, International Conference on Hydrogen Safety, Pisa, Italy, 2005.
[16] R. D. McCarthy, *Hydrogen: its technology and implications*, vol. III. CRC Press, 1975.
[17] B.-Z. Maytal, "Real gas choked flow conditions at low reduced-temperatures," *Cryogenics*, vol. 46, no. 1, pp. 21-29, Jan. 2006.
[18] B.-Z. Maytal and E. Elias, "Two-phase choking conditions of real gases flow at their critical stagnation temperatures and closely above," *Cryogenics*, vol. 49, no. 9, pp. 469-481, Sep. 2009.
[19] E. W. Lemmon, M. L. Huber, and M. O. McLinden, "NIST Standard Reference Database 23: Reference Fluid Thermodynamic and Transport Properties-REFPROP." National Institute of Standards and Technology, Standard Reference Data Program, , Gaithersburg, 2007.
[20] "Code of Federal Regulations, Department of Transportation (CFR-DOT), 1996a, 'Basic Requirements for Fully Wrapped Carbon Fiber Reinforced Aluminum Lined Cylinders,' Title 49, CFR107.105 Standard.".